Quantifying the Dependence of Westerly Wind Bursts on the Large-Scale Tropical Pacific SST

ELI TZIPERMAN

Department of Earth and Planetary Sciences, and Division of Engineering and Applied Sciences, Harvard University, Cambridge, Massachusetts

LISAN YU

Department of Physical Oceanography, Woods Hole Oceanographic Institution, Woods Hole, Massachusetts

(Manuscript received 5 June 2005, in final form 17 October 2006)

ABSTRACT

The correlation between parameters characterizing observed westerly wind bursts (WWBs) in the equatorial Pacific and the large-scale SST is analyzed using singular value decomposition. The WWB parameters include the amplitude, location, scale, and probability of occurrence for a given SST distribution rather than the wind stress itself. This approach therefore allows for a nonlinear relationship between the SST and the wind signal of the WWBs. It is found that about half of the variance of the WWB parameters is explained by only two large-scale SST modes. The first mode represents a developed El Niño event, while the second mode represents the seasonal cycle. More specifically, the central longitude of WWBs, their longitudinal extent, and their probability seem to be determined to a significant degree by the ENSO-driven signal. The amplitude of the WWBs is found to be strongly influenced by the phase of the seasonal cycle. It is concluded that the WWBs, while partially stochastic, seem an inherent part of the large-scale deterministic ENSO dynamics. Implications for ENSO predictability and prediction are discussed.

1. Introduction

Westerly wind bursts in the equatorial Pacific may be defined as wind events with speed larger than, say, 4 $m\,s^{-1}$ and lasting at least a few days. These events are known to play an important role in ENSO's dynamics, and in particular during ENSO's onset (e.g., Lau and Chan 1988; Lengaigne et al. 2004; McPhaden 1999). These events seem to result from various mechanisms, from tropical cyclones (Keen 1982) to cold surges from midlatitudes (Chu 1988), the Madden–Julian oscillation (MJO; Chen et al. 1996; Zhang 1996), or some combination of the three (Yu and Rienecker 1998).

Westerly wind bursts (WWBs) are commonly considered external stochastic forcing for ENSO (e.g., Moore and Kleeman 1999) and were proposed to be close to the optimal stochastic forcing for ENSO (Moore and Kleeman 2001). However, it is known that WWBs occur more frequently during El Niño events (Delcroix et al. 1993; Harrison and Vecchi 1997; McPhaden 1999; Vecchi and Harrison 2000; Verbickas 1998; Yu et al. 2003). Also, Batstone and Hendon (2005) recently analyzed the atmospheric weather noise that is possibly related to MJO events and found that its variance shifts eastward during El Niño events. Vecchi and Harrison (2000) analyzed composites of the ocean sea surface temperatures when a WWB occurs, focusing on the composites of the change in SST induced by the WWBs. They found that in the absence of an El Niño event already in progress, WWBs tend to be preceded by a shift of the warm pool to the east. Vecchi et al. (2006) and Lengaigne et al. (2003) investigated the role of the SST forcing in the WWB enhancement at the onset of the 1997–98 El Niño.

Several of the above studies seem to suggest that the occurrence and characteristics of WWBs are influenced by the large-scale SST state as determined by ENSO itself. Eisenman et al. (2005) therefore examined the dynamical consequences of a modulation of the occurrence and characteristics of WWBs by the large-scale SST. They contrasted two scenarios using the Zebiak

Corresponding author address: Eli Tziperman, Department of Earth and Planetary Sciences, Harvard University, Cambridge, MA 02138-0000.
E-mail: eli@eps.harvard.edu

DOI: 10.1175/JCLI4138.1

and Cane (1987) ENSO model, one in which WWBs are completely stochastic and one in which their occurrence is a function of the extent of the warm pool. With the same average number of events per year in both scenarios, the modulation of the WWBs by the SST results in an ENSO amplitude twice as large as for completely stochastic WWBs. This was explained by Eisenman et al. (2005) to be a result of an enhancement of the slow component of the WWBs (Roulston and Neelin 2000) by the SST modulation. These results were reinforced using a fuller hybrid coupled model (ocean GCM coupled to a statistical atmospheric model) and allowing the WWBs to be partially stochastic (Gebbie et al. 2006). In a somewhat related modeling study, Perez et al. (2005), motivated by the view that WWBs may be a multiplicative noise forcing of ENSO, studied the difference in ENSO's response to additive versus multiplicative noise in an intermediate coupled model. (A multiplicative noise of a given dynamical system is a stochastic forcing term that appears in the equations such that it depends on the state of the system itself; for example, the amplitude of the noise could be proportional to the state. An additive noise is completely independent of the system state.)

Statistical atmospheric models commonly calculate the wind stress from the SST based on a singular value decomposition (SVD) of the covariance matrix of the two fields (Bretherton et al. 1992; Harrison et al. 2002; Syu and Neelin 2000b). The resulting wind field is large scale and slowly varying, like the SST itself, and does not include a representation of WWBs.

The objective of this paper is to analyze the link between the SST and the WWBs by using simple linear statistical analysis tools (SVD), yet without assuming a linear relationship between the wind at a given place and the SST. We do so by correlating the SST and the parameters governing the WWB characteristics, rather than the SST and the wind itself. By using this approach we allow for a nonlinear relationship between the SST and the wind signal of the WWBs in our analysis. We also allow for the fact that the WWBs are at least partially stochastic in our analysis.

Specifically, our objectives here are first to find out which SST patterns affect and modulate what aspects of the observed WWBs, and second to use this analysis to derive a procedure that allows the inclusion of WWBs in models that cannot resolve them explicitly, which is currently the case for all intermediate models as well as for some atmospheric GCMs.

The following sections introduce our methodology (section 2), the data (section 3), the results and interpretation (section 4), and the conclusions (section 5).

2. Methodology

Our objective is to investigate possible connections between the large-scale SST structure and the WWBs. Our approach is motivated by the standard SVD procedure for deriving a statistical atmosphere relating the wind to the SST (Bretherton et al. 1992; Harrison et al. 2002; Syu and Neelin 2000a; see also the regression approach of Batstone and Hendon 2005). However, rather than applying the SVD analysis to the correlation between the wind field and SST field, we apply it to the correlation between the parameters characterizing the WWBs on the one hand and the SST field on the other.

Suppose the WWBs are characterized by parameters in a $q \times 1$ vector that includes elements such as

$$\mathbf{R}(t) = (A, x_0, y_0, L_{\mathrm{EW}}, L_{\mathrm{NS}}, T, p)^{\mathrm{T}}, \tag{1}$$

corresponding to the amplitude, central longitude, central latitude, east–west extent, north–south extent, duration, and probability of occurrence. In our calculations, therefore, $q = 7$ and generally $q = N$, where N is the number of grid points at which the wind and SST observations are given. The above parameters allow us to characterize the main features of individual wind events, although not to completely reproduce all details of each individual event. Given these characteristics, the WWBs may be reconstructed, for example, as having an idealized Gaussian structure in space and time,

$$\tau = A \exp\left[-\frac{(x - x_0)^2}{L_{\mathrm{EW}}^2} - \frac{(y - y_0)^2}{L_{\mathrm{NS}}^2} - \frac{(t - t_0)^2}{T^2} \right]. \tag{2}$$

Alternatively, it is possible to use a composite spatial and temporal WWB structure based on observations and to set the scale and amplitude of the composite event using the above individual characteristics recorded for each event. Figure 1 shows an actual WWB event, together with its fit based on (2) and the parameters in (1). The idealized fit provides a reasonably good description of the actual event, showing that our set of chosen parameters is able to reproduce the WWB structure quite reasonably.

We consider here the possibility that the WWBs' amplitude, location, structure, and time of occurrence may be deterministically modulated by the large-scale SST. Yet, even if this is the case, there is still an important stochastic element to the WWBs. We bring this to account by including a parameter that represents the probability of occurrence, p, of a WWB for a given SST distribution. To evaluate this probability at a time t from the observations, we scan an interval of 3 months centered around t. The number of WWBs within this interval divided by 3 months is defined to be the prob-

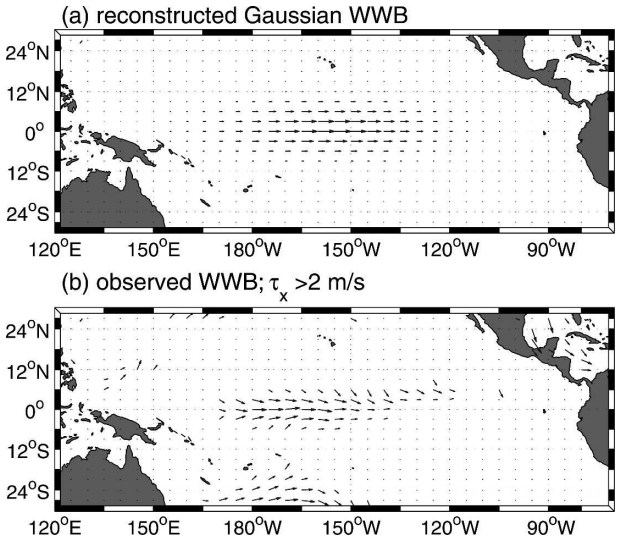

FIG. 1. (a) An idealized reconstruction of a WWB using Eq. (2) and the parameters in Eq. (1). (b) Wind vectors for an observed WWB event whose parameters are used to produce (a); the observed wind is averaged over 15–19 Oct 1997.

ability per month, p, for having a WWB at that time. We found that changing the interval length from 2 to 4 months does not change our results (e.g., the structure of the SST singular vectors) significantly.

Before analyzing the time series of the WWB parameter vector $\mathbf{R}(t)$, each element of this vector is nondimensionalized by removing its mean and dividing it by its standard deviation. Next, one defines the elements of the $N \times q$ correlation matrix $\mathbf{C}$ between the SST and the WWB parameters to be defined via the following average over the observations, which are given at N_{wwb} different times:

$$\mathbf{C}_{ij} = \frac{1}{N_{\text{wwb}} - 1} \sum_{t=1}^{N_{\text{wwb}}} T_i(t)\mathbf{R}_j(t). \tag{3}$$

Here, $T_i(t)$ is the SST at a location i (representing both latitude and longitude and varying over the entire tropical Pacific) and time t.

The singular values and right and left eigenvectors of the covariance matrix $\mathbf{C}$ satisfy

$$\mathbf{C}\mathbf{e}^{(R,i)} = \lambda_i \mathbf{e}^{(\text{SST},i)} \tag{4}$$

$$\mathbf{C}^{\text{T}}\mathbf{e}^{(\text{SST},i)} = \lambda_i \mathbf{e}^{(R,i)}, \tag{5}$$

where $\mathbf{e}^{(\text{SST},i)}$ is the ith SST vector and $\mathbf{e}^{(R,i)}$ the ith WWB parameter vector. Writing the singular values λ_i as the diagonal elements of a diagonal matrix $\mathbf{\Lambda}$ and the matrices of the eigenvectors as

$$\mathrm{e}^{(R)} = [\mathbf{e}^{(R,1)}, \ldots, \mathbf{e}^{(R,q)}] \tag{6}$$

$$\mathrm{e}^{(\text{SST})} = [\mathbf{e}^{(\text{SST},1)}, \ldots, \mathbf{e}^{(\text{SST},N)}], \tag{7}$$

the SVD decomposition is

$$\mathbf{C} = [\mathbf{e}^{(\text{SST})}]^{\text{T}}\mathbf{\Lambda}\mathbf{e}^{(R)}. \tag{8}$$

In the following, we will use these right and left eigenvectors of $\mathbf{C}$ to analyze the WWB–SST correlations. But let us first consider how the WWB–SST covariance as well as the WWB parameter variance described by a given SVD mode are calculated.

The fraction of the covariance explained by each mode, $f_{\text{covar}}(i)$, is given by

$$f_{\text{covar}}(i) = \lambda_i^2 / \sum_{j=1}^{q} \lambda_j^2. \tag{9}$$

To obtain the fraction of the variance of the WWB characteristics vector described by each SVD mode, reconstruct the WWB parameter time series using the principal components $r_i^{\text{wwb}}(t)$,

$$r_i^{\text{wwb}}(t) = [\mathbf{e}^{(R,i)}]^{\text{T}}\mathbf{R}(t). \tag{10}$$

Then, the fraction of the variance of the WWB characteristics vector, $\mathbf{R}(t)$, explained by a given WWB SVD vector is given by the ratio of the variance of the appropriate principal component $r_i^{\text{wwb}}(t)$ to the total variance of the WWB parameter vector, obtained by summing over all principal components,

$$f_{\text{variance,wwb}}(i) = \text{var}[r_i^{\text{wwb}}(t)] / \sum_{j=1}^{q} \text{var}[r_j^{\text{wwb}}(t)]. \tag{11}$$

The first few SST singular vectors contain the spatial SST structure that has the most effect on the WWB parameters. If we believe that the warm phase of ENSO plays a significant role in setting the timing and characteristics of the WWBs, then we expect one of the first singular vectors to reflect the structure of the El Niño SST warming. If the WWBs are not affected by the SST at all, we can expect the SVD vectors for the SST to be dominated by spatial noise rather than a coherent large-scale structure. We will see below that a useful signal can be extracted in the present case, indicating that the SST plays a significant role in determining the WWB characteristics.

3. Data

The SST data used here are obtained from the optimal interpolation SST (OISST) version-2 analysis (Reynolds et al. 2002). The analysis uses in situ and satellite Advanced Very High Resolution Radiometer (AVHRR) SSTs to produce a weekly field on a 1° grid from 25°S to 25°N in the Pacific Ocean. The dataset is available from November 1981 onward. The SST data used in the analysis here were first subsampled to a

resolution of 2° in both latitude and longitude. The surface wind dataset is the (special sensor microwave/imager) SSM/I-derived winds over the oceans produced by Atlas et al. (1996). A two-dimensional variational analysis method was used to combine information from the European Centre for Medium-Range Weather Forecasts (ECMWF) 10-m surface wind analyses, SSM/I wind speeds, and ship and buoy winds to produce new 1° gridded surface wind analyses for every 6 h starting in July 1987.

Using the 6-hourly wind data, we created a time series of WWB characteristics for the parameters in (1). A WWB event is defined for this purpose by (i) an amplitude of zonal wind anomalies greater than 5m s^{-1}, (ii) a duration greater than 2 days and less than 40 days, (iii) a longitude extension greater than 500 km, and (iv) latitude extension being measured at the time when the longitude extension is at maximum. The precise WWB definition is necessarily arbitrary to some degree. A total of 127 events were identified for the period of 1988–2005, at a yearly average of 7.5 events per year—about twice the rate found by Eisenman et al. (2005) using a different definition.

The time series for the WWB parameters are shown in Fig. 2 together with the Niño-3 index for this time period. While it is difficult to find significant correlations of the WWB parameters with the Niño-3 index, it still seems from the figure that these parameters respond to the phase of ENSO and therefore possibly to the SST as well. This is especially apparent during the strong 1997 event. At that time the WWBs became longer, stronger, and more frequent, their central longitude migrated eastward during the development of the El Niño event, and their east–west and north–south extents seemed to get larger. These are only preliminary impressions to be quantified by the analysis to follow, and we would be particularly interested in which SST structures specifically result in a change to which of the WWB parameters.

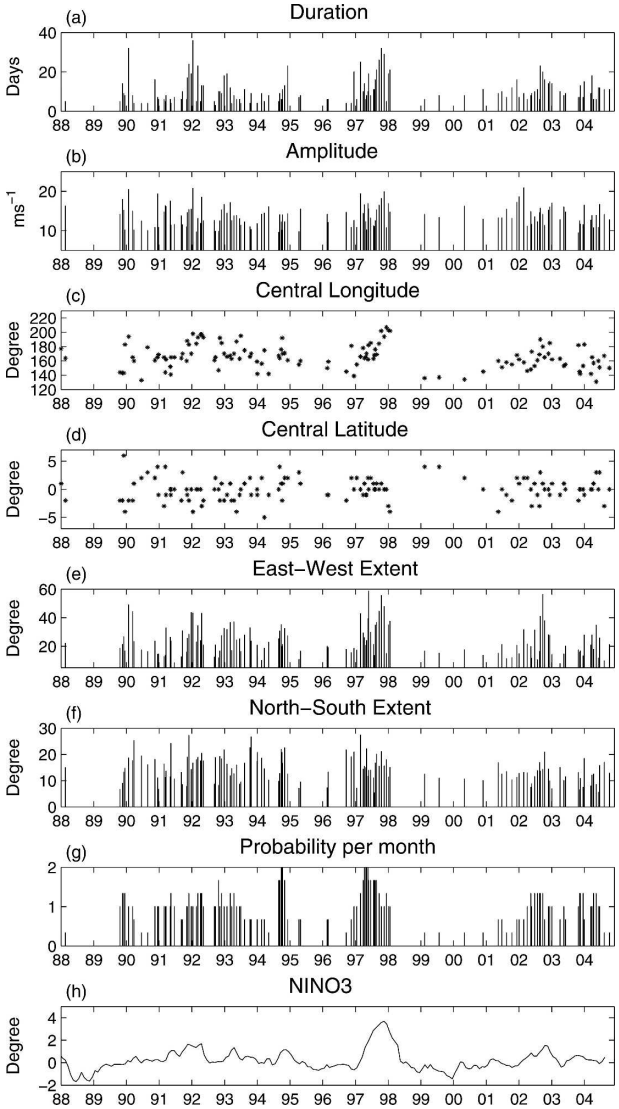

FIG. 2. (a)–(g) Time series of the different parameters characterizing the WWB events [see explanation of Eq. (1) in text] and the (h) Niño-3 index as a function of time.

4. Results

The first three SST SVD vectors are shown in Fig. 3, and all seven WWB SVD vectors are given in Table 1. The results show a dependence of the WWB parameters on the large-scale SST. The first SVD vector pair [$\mathbf{e}^{(\mathrm{SST},\,1)}$ and $\mathbf{e}^{(R,\,1)}$; see Eq. (4)] accounts for 56% of the covariance between the WWB parameters and the SST [see Eq. (9); Table 1; Fig. 3]. This first WWB SVD vector [$\mathbf{e}^{(R,\,1)}$] also accounts for 34% of the variance of the WWB parameter vector time series (11). To interpret the WWB SVD vectors, we note that a WWB SVD vector with a single element equal to one and the rest being zero would imply that the SST structure shown by the corresponding SST SVD vector completely determines the WWB parameter corresponding to the one nonzero entry.

In the present case, the first SVD WWB vector (Table 1) contains several nonzero elements, indicating that the SST structure shown by the first SST SVD vector determines a linear combination of the WWB parameters. The dominant WWB parameters in this first vector are those corresponding to the center longitude of the wind events, x_0, their east–west extent, L_{EW}, and the probability of occurrence, p. Given that the spatial structure of the first SST SVD vector reflects that of a warm El Niño event, we conclude that these

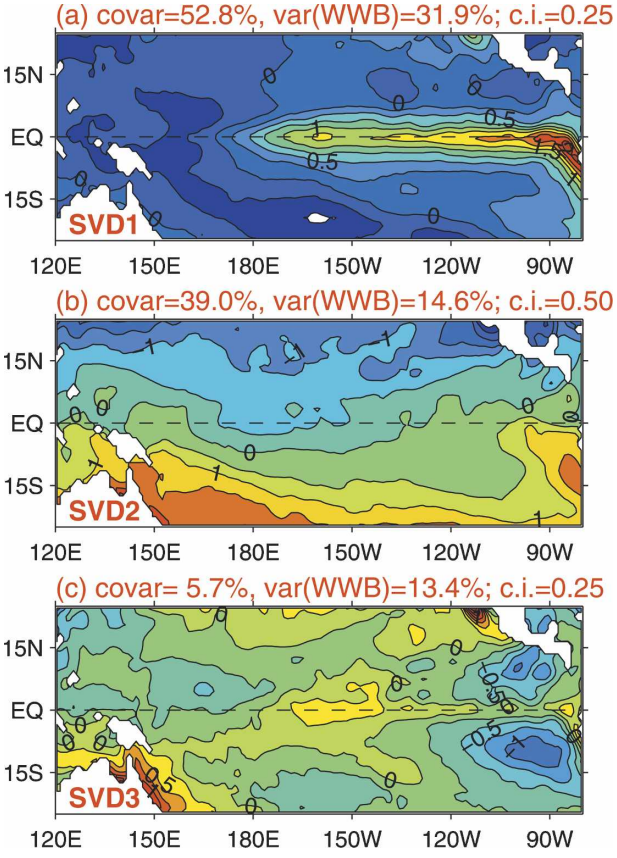

FIG. 3. The (a)–(c) first three SST SVD vectors [$\mathbf{e}^{(SST,\,i)}$, Eq. (4)] from the analysis of the covariance matrix between the WWB parameters and the SST. The labels of (a)–(c) show the covariance between the SST and WWB parameters described by each mode [Eq. (9)], the portion of the WWB parameter variance explained by each mode [Eq. (11)], and the contour interval. The SST SVD vectors are each normalized by the std dev of the corresponding principal component.

TABLE 1. The first seven rows of this table give the seven SVD vectors for the WWB parameters shown in Eq. (1). The entries are all multiplied by 100. The row marked "%covar" contains the percentage of the covariance between the SST and the WWB parameters explained by each SVD vector [using the singular values, Eq. (9)]. The last row, marked "%var(τ)," is the percentage of the variance of the WWB parameter vector explained by each SVD vector [using Eq. (11)].

	1	2	3	4	5	6	7
A	18	81	2	35	0	2	43
x_0	58	−20	27	−49	−23	0	51
L_{EW}	49	4	−7	17	−11	−75	−39
L_{NS}	11	−13	31	6	91	−15	14
T	27	1	67	30	−14	43	−43
P	47	−33	−56	43	11	38	8
y_0	−28	−41	27	57	−27	−29	44
%covar	53	39	6	1	1	0	0
%var(τ)	32	15	13	15	12	7	6

three WWB parameters are very strongly linked to the occurrence of a warm event in the equatorial Pacific.

The second WWB SVD vector is dominated by the entry corresponding to the amplitude of the WWB event, A. The second SST vector has a structure with a north–south gradient, reflecting the seasonal cycle and the tendency of the events to be stronger during the boreal winter. We conclude that the seasonal cycle is the most important factor determining the amplitude of WWBs. The second WWB vector also seems to determine the central latitude of the event. This component is negative (−0.41), indicating [given the structure of the corresponding second SST SVD mode (Fig. 3)] that the events tend to happen in the Southern Hemisphere during the Northern Hemisphere winter. This may be related to the seasonal characteristics of intraseasonal convection anomalies (Madden–Julian oscillation; Wang and Rui 1990), which seem to be among the factors leading to WWBs. Off-equatorial wind events were proposed to play an important role in ENSO's dynamics (Vecchi and Harrison 2003). This makes the correlation between the WWB latitude and SST especially relevant in case one wishes to use our formulation for representing WWBs in ENSO models. On the other hand, the second singular SST vector has practically no effect on the duration of the WWB events (entry corresponding to T in Table 1 is only 0.01), indicating that our analysis is not able to find a connection between seasonality and the duration of the events.

The third SVD vector pair only accounts for 6% of the covariance between the WWB parameters and the SST, although it does account for 13% of the WWB parameter vector variance. The large-scale structure of this mode suggests that physical interpretation in this case may be possible (and perhaps related to the off-equatorial SST signal in the east Pacific), but its value is questionable given that the covariance explained by this vector is very small. The rest of the SVD vectors account for negligible parts of the covariance between the WWBs and the SST, and their spatial structure tends to be dominated by noise. It is quite remarkable that the first two SVD SST vectors reflect large-scale SST changes and account for so much of the covariance (92%) and of the WWB parameter variance (47.0%). This reflects a clear dependence of the WWBs on the large-scale SST. This indicates that the WWBs should probably not be considered external noise, but that a large part of their variance is, in fact, explained by the large-scale SST, specifically by El Niño and the seasonal cycle.

Our analysis differs from previous efforts to analyze the WWB–SST correlations in two critical ways. First, we explicitly included the partially stochastic nature of

TABLE 2. A summary of the different ways used to extract WWBs from the wind data and the results of the corresponding correlation analyses with the SST.

Case parameters	0	1	2	3
WWBs from parameters	y	n	n	n
Remove SVD correlations	n	y	y	n
Remove below threshold	n	n	y	y
Remove above threshold	n	n	n	n
Threshold value (m s^{-1})	—	—	0	4
Results				
Covar explained by 2 modes	0.93	0.41	0.97	0.95
Covar explained by 8 modes	1	0.91	1	1
Var explained by 2 modes	0.48	0.06	0.1	0.24
Var explained by 8 modes	0.9	0.34	0.29	0.5
Figure	4a	4b	4c	4d

the WWBs by including a probability measure p. This enables the analysis to find a link between the SST and the WWBs even if the specific time of each given WWB cannot be traced to a specific feature of the SST. Second, our set of WWB parameters is nonlinearly related to the wind stress field itself. Consider, for example, the expression for the idealized Gaussian WWB in (2). The relations between the wind field on the one hand and the period of the WWB, its location, or spatial extent on the other are all nonlinear. While our analysis searches for a linear correlation between the WWB parameters and the SST, it still allows for a nonlinear relation between the WWB wind field and the large-scale SST. This may have resulted in correlations between the wind bursts and SST reported above which could perhaps not be found in a purely linear SVD analysis of the covariance of the wind field and the SST.

To put the above results in perspective, we extracted estimates for the WWBs from the wind data in several different ways that are used in previous studies. These different cases are summarized in Table 2 and the corresponding estimated WWB wind fields are shown in Fig. 4.

We begin by constructing a parameterized WWB

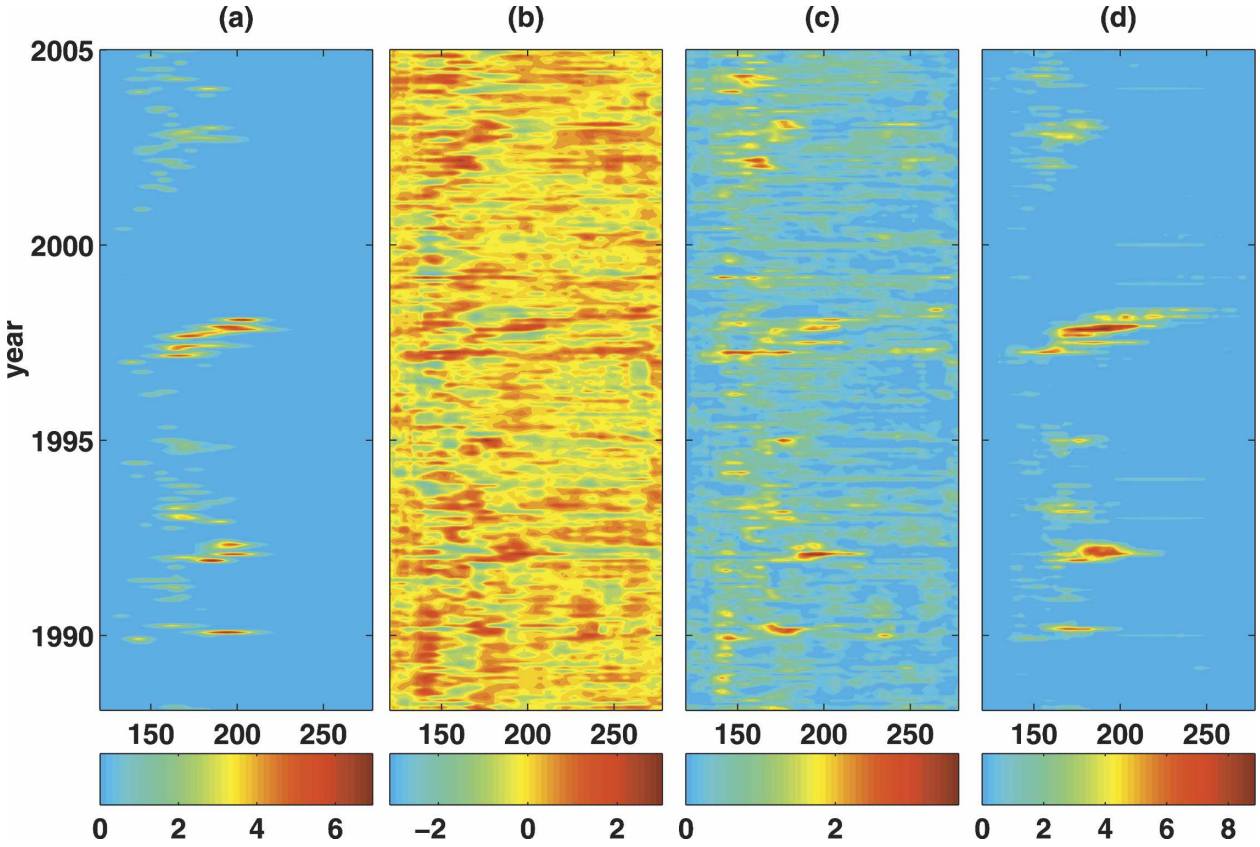

FIG. 4. Hovmöller plot of the WWBs extracted from the wind data in the different ways summarized by Table 2: (a) wind reconstructed from our time series of WWB characteristics assuming an idealized Gaussian structure in space and time; (b) wind residuals after removing the first eight SVD modes of the autocorrelation between the wind and SST; (c) same as (b), but with the negative wind anomalies discarded; and (d) showing only winds above 4 m s^{-1}, with wind speed at other locations set to zero. Shown are contours of the equatorial zonal wind speed as a function of time and longitude.

wind field by adding up the Gaussian wind bursts (2) based on our WWB parameters time series (1). This WWB wind field is a function of space and time and we proceed by analyzing the SVD of its $N \times N$ covariance matrix with the SST. We find that the first two SVD modes account for 93% of the covariance between this wind field and the SST, and—more importantly—for 48% of the wind field variance (case 0; Table 2). These are very similar results to those we obtained when we analyzed the covariance matrix of the WWB parameters and the SST. Eight SVD modes account for 90% of the wind variance, indicating that this WWB wind field is strongly correlated with the SST, in support of the previous analysis of the parameter vector time series.

Returning to the observed wind stress, we proceed (case 1 in Table 2) to calculate the SVD correlation between the SST and the total wind stress, and remove the first 8 modes from the wind field that describe over 99% of the covariance between the 2 fields. The resulting residual wind field is mostly small scale and high frequency (Fig. 4b). This residual field is, of course, not well correlated with the SST. Calculating the correlation matrix between this residual wind and the SST and performing an SVD analysis of this matrix, we find that the first 2 SVD modes account for 93% of the remaining covariance between the wind residuals and SST but only for 6% of the variance of the wind signal. Eight modes account for 34% of the variance in this case. We conclude that the portion of the wind residual variance that is correlated with the SST is negligible, as expected. While this residual wind field is not correlated with the SST, it also does not have the characteristics of the observed major WWBs (cf. Figs. 4a,b).

Next (case 2), we repeat the above procedure of removing the first eight SVD modes from the wind field but then also proceed to remove the negative portion of the remaining residual wind stress signal, leaving only positive (westerly) winds. The resulting wind field (Fig. 4c) is still not significantly correlated with the SST field as seen in Table 2, nor does it have the observed WWB structure, supporting the final conclusion of case 1.

Next (case 3), we crudely define the WWBs to involve all data points at which the weekly averaged zonal wind speed exceeds 4 m s^{-1}. The resulting wind field is shown in Fig. 4d. This time, this WWB estimate does have the characteristic WWB structure in space and time, and it is also much better correlated with the large-scale SST. The first 2 SVD modes between the wind field with speed above 4 m s^{-1} and the SST account for 97% of the covariance with the SST and for 24% of the wind variance. Eight modes account for 50% of the wind variance. This is a significantly larger portion of the variance than that explained in cases 1 and 2, and this time the estimated wind field does have the structure of the observed major WWBs.

There are further analyses that were not considered here but that could be interesting to perform. For example, one could consider the effect of the SST only on equatorial WWBs that presumably play an especially important role in ENSO's dynamics. Also, it may be interesting to isolate the effect of specific ENSO events on the analysis, such as the dominant 1997 El Niño.

5. Conclusions

We attempted to examine and quantitatively characterize the correlations between the equatorial Pacific westerly wind bursts (WWBs) and the large-scale SST. Our approach was to extract from the raw 6-hourly wind data a time series of parameters characterizing the WWBs' amplitude, location, spatial and temporal extent, and probability of occurrence. We then correlated this time series with the SST using a singular value decomposition analysis of the correlation matrix. The advantage of our approach is that it allows for the nonlinear dependence between the wind field of the WWBs and the SST, as well as for the partially stochastic nature of the WWBs. That is, we analyzed the linear correlation of the WWB parameters and the SST, but the WWB parameters are nonlinearly related to the WWB field itself. So we effectively allowed for a nonlinear relation between the SST and the WWB wind field.

We contrasted our analysis with alternative ways for estimating the WWB field and concluded that when the extracted wind field has the main characteristics of significant WWBs, it is significantly correlated with the large-scale SST. On the other hand, when we construct a WWB estimate by removing the portion of the wind field that is correlated with the SST, we are left with "noise" that is not correlated but that also does not have the main characteristics of major WWB events. We conclude that the main WWB signal is significantly correlated with the SST.

By explicitly correlating the parameters governing the WWBs with the SST, we also find which SST structure governs each of the WWB parameters. We find that ENSO and the seasonal cycle dominate the characteristics of the WWBs. The central longitude of the WWB events, their longitudinal extent, and their probability of occurrence are all determined to a significant degree by the ENSO-driven SST signal. The amplitude of the wind bursts is found to be strongly influenced by the phase of the seasonal cycle. This very specific information comes very naturally out of the SVD analysis of the covariance matrix of the WWB characteristics

and the SST. The correlation between the WWBs and the SST field cannot, unfortunately, be considered conclusive because of the short time period for which high-quality wind observations are available. These results are still interesting and it is worth considering their implications. A more conclusive study would require wind data that extend over more WWBs, and in particular over more ENSO events, to allow extracting a more statistically significant relation between WWBs and SST.

WWBs have been mostly treated as stochastic noise that is external to the equatorial Pacific and ENSO, and this became a significant part of the view of ENSO as a damped oscillator driven by external noise (e.g., Kleeman and Moore 1997; Moore and Kleeman 2001; Penland and Sardeshmukh 1995). In contrast, Eisenman et al. (2005) and Gebbie et al. (2006) examined the consequences of the possibility that the WWBs' occurrence and characteristics are partially modulated by the SST. They find that such a partially deterministic modulation has a very significant effect on ENSO's amplitude and other characteristics. Our results here support the view that the WWBs are affected to a significant degree by the SST, and that they are therefore not a purely stochastic noise external to ENSO's dynamics.

One may term the WWBs' effects on ENSO "multiplicative noise" because they are strongly affected by the state of the equatorial Pacific, yet have a partial stochastic character (Perez et al. 2005). While this is technically correct, the stochastic element of the WWBs may not be very dominant in so far as ENSO's dynamics are concerned. Given the appropriate SST structure, a WWB is likely to occur. The chaotic weather dynamics or perhaps some unknown MJO dynamics may result in some uncertainty regarding the precise date of occurrence and characteristics of the WWB. But this uncertainty may not matter significantly to the large-scale ENSO dynamics, possibly leaving open the question of ENSO's irregularity arising from large-scale chaotic dynamics (Jin et al. 1994; Tziperman et al. 1994, 1995) or due to stochastic forcing (Kleeman and Moore 1997; Penland and Sardeshmukh 1995).

The correlation between the WWBs and SST suggests, of course, the use of WWBs predicted from the SST in ENSO prediction models. Eisenman et al. (2005) found that when the WWBs are modulated by the SST, increasing their amplitude in an ENSO model is roughly equivalent to an enhanced ocean–atmosphere coupling coefficient. However, this does not mean that an appropriate WWB representation or parameterization may be replaced by enhancing the coupling coefficient. The WWBs occur only for an extended warm pool extent and during the appropriate phase of the seasonal cycle (see the SST SVD modes shown in Fig. 3). An enhanced coupling coefficient, in contrast, influences the ENSO cycle during all seasons and all ENSO phases. One may use our findings here, however, in order to formulate a statistical WWB parameterization that reproduces the amplitude and probability of occurrence of the WWBs given the SST field. Such parameterized WWBs may be used in ENSO prediction models whose atmospheric component cannot reproduce the WWBs.

Acknowledgments. We thank Ian Eisenman, Jeff Shaman, Jake Gebbie, Peter Huybers, Zhiming Kuang, and Brian Farrell for very useful discussions. Useful and detailed comments from two anonymous reviewers were very helpful in improving the presentation. Eli Tziperman is supported by the U.S. National Science Foundation Climate Dynamics Program Grant ATM-0351123 and by the McDonnell Foundation. Lisan Yu is supported by the NASA Ocean Vector Wind Science Team under JPL Contract 1216955 and NSF Climate Dynamics Grant ATM-0350266.

REFERENCES

Atlas, R., R. N. Hoffman, S. C. Bloom, J. C. Jusem, and J. Ardizzone, 1996: A multiyear global surface wind velocity dataset using SSM/I wind observations. *Bull. Amer. Meteor. Soc.,* **77,** 869–882.

Batstone, C., and H. H. Hendon, 2005: Characteristics of stochastic variability associated with ENSO and the role of the MJO. *J. Climate,* **18,** 1773–1789.

Bretherton, C. S., C. Smith, and J. M. Wallace, 1992: An intercomparison of methods for finding coupled patterns in climate data. *J. Climate,* **5,** 541–560.

Chen, S. S., R. A. Houze Jr., and B. E. Mapes, 1996: Multiscale variability of deep convection in relation to large-scale circulation in TOGA COARE. *J. Atmos. Sci.,* **53,** 1380–1409.

Chu, P.-S., 1988: Extratropical forcing and the burst of equatorial westerlies in the western Pacific: A synoptic study. *J. Meteor. Soc. Japan,* **66,** 549–563.

Delcroix, T., G. Eldin, M. McPhaden, and A. Morlière, 1993: Effects of westerly wind bursts upon the western equatorial Pacific Ocean, February–April 1991. *J. Geophys. Res.,* **98** (C9), 16 379–16 385.

Eisenman, I., L. Yu, and E. Tziperman, 2005: Westerly wind bursts: ENSO's tail rather than the dog? *J. Climate,* **18,** 5224–5238.

Gebbie, G., I. Eisenman, A. Wittenberg, and E. Tziperman, 2007: Modulation of westerly wind bursts by sea surface temperature: A semi-stochastic feedback for ENSO. *J. Atmos. Sci.,* in press.

Harrison, D. E., and G. A. Vecchi, 1997: Westerly wind events in the tropical Pacific, 1986–95. *J. Climate,* **10,** 3131–3156.

Harrison, M. J., A. Rosati, B. J. Soden, E. Galanti, and E. Tziperman, 2002: An evaluation of air–sea flux products for ENSO simulation and prediction. *Mon. Wea. Rev.,* **130,** 723–732.

Jin, F.-F., D. Neelin, and M. Ghil, 1994: ENSO on the devil's staircase. *Science,* **264,** 70–72.

Keen, R. A., 1982: The role of cross-equatorial tropical cyclone pairs in the Southern Oscillation. *Mon. Wea. Rev.,* **110,** 1405–1416.

Kleeman, R., and A. M. Moore, 1997: A theory for the limitation of ENSO predictability due to stochastic atmospheric transients. *J. Atmos. Sci.,* **54,** 753–767.

Lau, K. M., and P. H. Chan, 1988: Intraseasonal and interannual variations of tropical convection: A possible link between the 40–50 day oscillation and ENSO. *J. Atmos. Sci.,* **45,** 506–521.

Lengaigne, M., J.-P. Boulanger, C. Menkes, G. Madec, P. Delecluse, E. Guilyardi, and J. Slingo, 2003: The March 1997 Westerly Wind Event and the onset of the 1997/98 El Niño: Understanding the role of the atmospheric response. *J. Climate,* **16,** 3330–3343.

——, E. Guilyardi, J.-P. Boulanger, C. Menkes, P. Delecluse, P. Inness, J. Cole, and J. Slingo, 2004: Triggering of El Niño by westerly wind events in a coupled general circulation model. *Climate Dyn.,* **23,** 601–620.

McPhaden, M. J., 1999: Climate oscillations-genesis and evolution of the 1997–98 El Niño. *Science,* **283,** 950–954.

Moore, A. M., and R. Kleeman, 1999: Stochastic forcing of ENSO by the intraseasonal oscillation. *J. Climate,* **12,** 1199–1220.

——, and ——, 2001: The differences between the optimal perturbations of coupled models of ENSO. *J. Climate,* **14,** 138–163.

Penland, C., and P. D. Sardeshmukh, 1995: The optimal growth of tropical sea surface temperature anomalies. *J. Climate,* **8,** 1999–2024.

Perez, C. L., A. M. Moore, J. Zavala-Garay, and R. Kleeman, 2005: A comparison of the influence of additive and multiplicative stochastic forcing on a coupled model of ENSO. *J. Climate,* **18,** 5066–5085.

Reynolds, R. W., N. A. Rayner, T. M. Smith, D. C. Stokes, and W. Wang, 2002: An improved in situ and satellite SST analysis for climate. *J. Climate,* **15,** 1609–1625.

Roulston, M. S., and J. D. Neelin, 2000: The response of an ENSO model to climate noise, weather noise and intraseasonal forcing. *Geophys. Res. Lett.,* **27,** 3723–3726.

Syu, H. H., and J. D. Neelin, 2000a: ENSO in a hybrid coupled model. Part I: Sensitivity to physical parameterizations. *Climate Dyn.,* **16,** 19–34.

——, and ——, 2000b: ENSO in a hybrid coupled model. Part II: Prediction with piggyback data assimilation. *Climate Dyn.,* **16,** 35–48.

Tziperman, E., L. Stone, M. A. Cane, and H. Jarosh, 1994: El-Niño chaos: Overlapping of resonances between the seasonal cycle and the Pacific Ocean-atmosphere oscillator. *Science,* **264,** 72–74.

——, M. A. Cane, and S. E. Zebiak, 1995: Irregularity and locking to the seasonal cycle in an ENSO prediction model as explained by the quasi-periodicity route to chaos. *J. Atmos. Sci.,* **52,** 293–306.

Vecchi, G. A., and D. E. Harrison, 2000: Tropical Pacific sea surface temperature anomalies, El Niño, and equatorial westerly wind events. *J. Climate,* **13,** 1814–1830.

——, and ——, 2003: On the termination of the 2002–03 El Niño event. *Geophys. Res. Lett.,* **30,** 1964, doi:10.1029/2003GL017564.

——, A. T. Wittenberg, and A. Rosati, 2006: Reassessing the role of stochastic forcing in the 1997–98 El Niño. *Geophys. Res. Lett.,* **33,** L01706, doi:10.1029/2005GL024738.

Verbickas, S., 1998: Westerly wind bursts in the tropical Pacific. *Weather,* **53,** 282–284.

Wang, B., and H. Rui, 1990: Synoptic climatology of transient tropical intraseasonal convection anomalies: 1975–1985. *Meteor. Atmos. Phys.,* **44** (1–4), 43–61.

Yu, L., and M. M. Rienecker, 1998: Evidence of an extratropical atmospheric influence during the onset of the 1997–98 El Niño. *Geophys. Res. Lett.,* **25,** 3537–3540.

——, R. A. Weller, and T. W. Liu, 2003: Case analysis of a role of ENSO in regulating the generation of westerly wind bursts in the Western Equatorial Pacific. *J. Geophys. Res.,* **108,** 3128, doi:10.1029/2002JC001498.

Zebiak, S. E., and M. A. Cane, 1987: A model El Niño–Southern Oscillation. *Mon. Wea. Rev.,* **115,** 2262–2278.

Zhang, C. D., 1996: Atmospheric intraseasonal variability at the surface in the tropical western Pacific Ocean. *J. Atmos. Sci.,* **53,** 739–758.